

横观各向同性基体复合材料的等效弹性常数*

张春春, 王艳超, 黄争鸣

(同济大学 航空航天与力学学院, 上海 200092)

(本刊编委黄争鸣来稿)

摘要: 细观力学的一个主要研究内容是求复合材料的等效弹性性能. 常见的细观力学模型解析公式一般假定基体各向同性且只存在纤维和基体两相材料, 实际复合材料的基体和纤维之间往往存在一个横观各向同性的界面相, 该三相复合材料的等效性能可由两个两相复合材料性能的组合得到, 这就需要求出横观各向同性基体复合材料的等效弹性常数. 该文基于两相同心圆柱模型, 首先导出了横观各向同性基体内应力与增强纤维内应力之间桥联矩阵的解析公式, 与基于数值积分 Eshelby 张量得到的 Mori-Tanaka 桥联矩阵相符, 再进一步获得了横观各向同性基体复合材料的 5 个弹性常数显式表达式. 文中还给出了扩展的桥联模型显式公式. 选用适当的桥联参数, 两种模型所得结果十分接近.

关键词: 细观力学; 等效弹性常数; 各向异性基体; 桥联矩阵; 桥联模型

中图分类号: TB123

文献标志码: A

DOI: 10.21656/1000-0887.380267

引 言

复合材料在工程中的应用越来越广泛, 在航空航天领域尤为重要. 掌握其力学性能是有效应用的前提. 细观力学研究的一个主要内容, 是根据组分材料纤维和基体的性能, 预测复合材料的等效弹性性能^[1-2]. 截止目前, 前人已建立起预测复合材料等效弹性性能的众多理论模型, 例如混合法^[3]、自洽模型^[4-5]、广义自洽模型^[6-7]、Mori-Tanaka 模型^[8]、Chamis 模型^[9]、桥联模型^[10]等. 但现有模型的解析公式, 一般是在基体为各向同性条件上建立起来的, 并且假定纤维和基体之间界面理想, 即只存在两相组分材料. 然而, 当在纤维和基体之间存在第三相材料如纤维表面涂层^[11-12], 或在纤维表面接枝纳米管进行复合材料增韧时^[13], 复合材料的纤维和基体之间往往生成一个横观各向同性的界面相, 其力学性能分析依赖于三相细观力学模型. 三相细观力学模型的应力场甚为复杂^[14], 一般难以得到显式表达式. 但仿照文献[15]中的等效纤维法, 可通过两次两相复合材料等效性能组合, 足够精确地求解三相复合材料的等效性能. 因此, 首先需要得到纤维增强横观各向同性基体单向复合材料的等效弹性常数公式. 2014 年, Grebenyuk 给出了基体为横观各向同性复合材料的轴向剪切模量的解析公式^[16], 但其他 4 个弹性常数的解析公式尚未见到. 本文目的在于补全其他 4 个解析公式.

* 收稿日期: 2017-09-28; 修订日期: 2018-05-23

基金项目: 国家自然科学基金(11472192; 11272238)

作者简介: 张春春(1993—), 女, 硕士生(E-mail: 532326775@qq.com);

黄争鸣(1957—), 男, 教授, 博士, 博士生导师(通讯作者. Tel: +86-21-65985373; E-mail: huangzm@tongji.edu.cn).

一般来说,自洽法和 Mori-Tanaka 方法可应用于基体为横观各向同性的情形,但这两种模型的建立都需要相应的 Eshelby 张量,形式复杂^[17-18]。另一方面,文献[19]中指出,可根据同心圆柱(CCA,即无限大基体夹无限长圆柱纤维)模型导出 Mori-Tanaka 的桥联矩阵,避免了直接求 Eshelby 张量。本文参考文献[19],在横观各向同性基体的 CCA 模型边界上,分别施加 6 种不同载荷,得到纤维和基体中的应力场,再相对各自体积均值化,使之满足均值应力的桥联方程。联立求解,得到基体为横观各向同性条件下的桥联矩阵,进一步可导出复合材料的 5 个等效弹性常数显式表达式,其中的轴向剪切模量公式与文献[16]相同。文中还对桥联模型进行了扩展,使其适用于横观各向同性基体的复合材料性能计算。通过对各复合材料等效弹性常数的计算对比,证实了当桥联参数取特定值时,由 CCA 模型和桥联模型计算的横观各向同性基体复合材料的各弹性参数十分接近。

1 桥联矩阵

实际材料皆非均质,须将应力相对单元体取平均后定义。复合材料中的单元体为代表性单元(RVE),相对 RVE 均质化,得应力应变的基本方程^[20]:

$$\{\sigma_i\} = V_f \{\sigma_i^f\} + V_m \{\sigma_i^m\}, \quad (1)$$

$$\{\varepsilon_i\} = V_f \{\varepsilon_i^f\} + V_m \{\varepsilon_i^m\}, \quad (2)$$

$$\{\varepsilon_i^f\} = [S_{ij}^f] \{\sigma_j^f\}, \quad (3)$$

$$\{\varepsilon_i^m\} = [S_{ij}^m] \{\sigma_j^m\}, \quad (4)$$

$$\{\varepsilon_i\} = [S_{ij}] \{\sigma_j\}, \quad (5)$$

其中上下标 f,m 分别代表纤维和基体,无上下标的表示复合材料, V_f, V_m 分别是纤维和基体体积含量, $V_f + V_m = 1$, $[S_{ij}]$ 表示柔度矩阵。

假定存在一个非奇异的桥联矩阵 $[A_{ij}]$, 使

$$\{\sigma_i^m\} = [A_{ij}] \{\sigma_j^f\}. \quad (6)$$

将式(6)代入式(1),求解得到纤维中的内应力:

$$\{\sigma_i^f\} = (V_f \mathbf{I} + V_m [A_{ij}])^{-1} \{\sigma_j\}, \quad (7)$$

式中, \mathbf{I} 是单位矩阵。再将式(7)代入式(6),得到基体的内应力:

$$\{\sigma_i^m\} = [A_{ij}] (V_f \mathbf{I} + V_m [A_{ij}])^{-1} \{\sigma_j\}. \quad (8)$$

进一步地,将式(7)和(8)代入式(3)和(4),再代入式(2),与式(5)对比,得单向复合材料柔度矩阵:

$$[S_{ij}] = (V_f [S_{ij}^f] + V_m [S_{ij}^m] [A_{ij}]) (V_f \mathbf{I} + V_m [A_{ij}])^{-1}. \quad (9)$$

在弹性范围内,正应力与剪应力互不耦合,桥联矩阵具有如下形式:

$$[A_{ij}] = \begin{bmatrix} A_{11} & A_{12} & A_{13} & 0 & 0 & 0 \\ A_{21} & A_{22} & A_{23} & 0 & 0 & 0 \\ A_{31} & A_{32} & A_{33} & 0 & 0 & 0 \\ 0 & 0 & 0 & A_{44} & A_{45} & A_{46} \\ 0 & 0 & 0 & A_{54} & A_{55} & A_{56} \\ 0 & 0 & 0 & A_{64} & A_{65} & A_{66} \end{bmatrix}. \quad (10)$$

由于方程(6)对任意载荷引起的基体和纤维均值应力场皆成立,只需选择 6 组线性无关外载,依次求出纤维和基体相对各自体积平均后的内应力,令它们满足方程(6),由此解出桥联矩阵。

2 纤维和基体应力及均值化

仿照文献[19],选横向剪切、轴向剪切 y (垂直于 y 轴的截面施加载荷)、轴向剪切 x (垂直于 x 轴的截面施加载荷)、轴向拉伸、双轴横向拉伸、单轴横向拉伸6组加载方式,求出纤维和基体中对应的应力,6组加载方式示意图如图1~6所示。

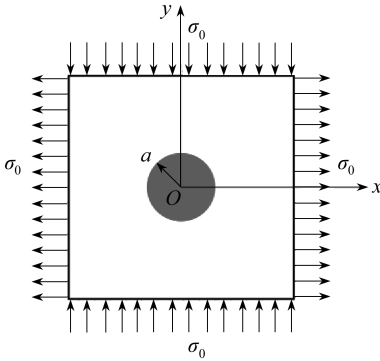


图1 横向剪切

Fig. 1 Transverse shearing

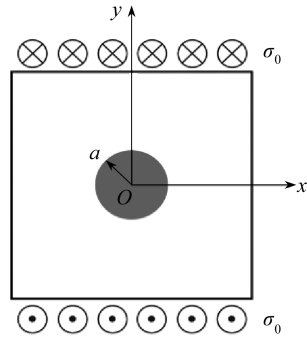


图2 轴向剪切 y (垂直于 y 轴)

Fig. 2 Longitudinal shearing in y and z plane

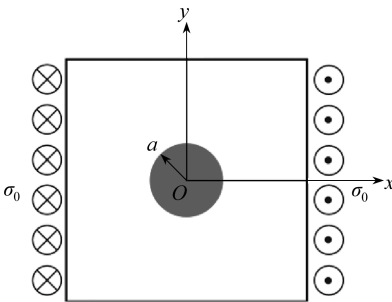


图3 轴向剪切 x (垂直于 x 轴)

Fig. 3 Longitudinal shearing in x and z plane

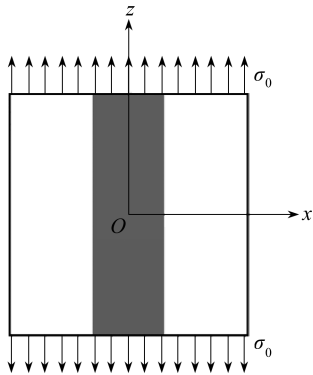


图4 轴向拉伸

Fig. 4 Longitudinal tension

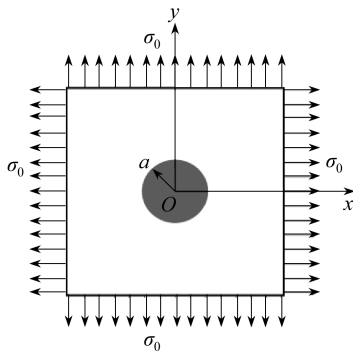


图5 双轴横向拉伸

Fig. 5 Biaxially transverse tension

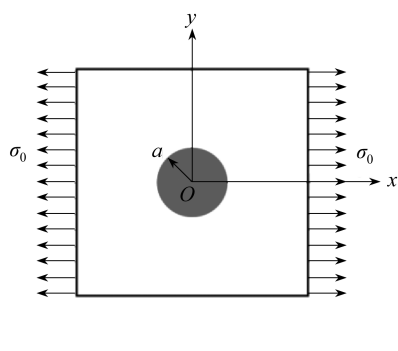


图6 单轴横向拉伸

Fig. 6 Uniaxially transverse tension

从文献[21-23]分别提取无限大基体夹单根无限长圆柱纤维模型下的横向剪切、轴向剪切、 y (垂直于 y 轴的截面施加载荷)、轴向拉伸、双轴横向拉伸的纤维和基体位移场试函数。位移场中的待定系数,通过纤维和基体径向应力和径向位移连续性条件以及无穷远处的应力边界条件确定。利用弹性力学的几何方程和物理方程^[24],求得相应的纤维和基体应力场。

经坐标变换,将柱坐标下的应力场转换到直角坐标下的应力场,并将纤维和基体应力场相对各自体积积分,再除以体积得平均应力。纤维圆柱体,基体为无限大空心圆柱。由于纤维和基体横截面面积及各自应力场均不随 z 坐标变化,平均应力的公式如下:

$$\overline{\sigma}_i^m = \frac{1}{\pi(b^2 - a^2)} \int_a^b \int_0^{2\pi} \sigma_i^m r dr d\theta, \quad (11)$$

$$\overline{\sigma}_i^f = \frac{1}{\pi a^2} \int_0^a \int_0^{2\pi} \sigma_i^f r dr d\theta, \quad (12)$$

式中,应力分量的下标 $i = x, y, z, xy, xz, yz$ 分别代表对应的正应力和剪应力, a 是纤维的半径, b 是基体的半径,且 $b \rightarrow \infty$ 。

1) 横向剪切

横向剪切可由 x 向的均匀拉伸和 y 向的等值均匀压缩产生。但若按图1计算,所得纤维和基体剪应力 $\sigma_{xy}, \sigma_{xz}, \sigma_{yz}$ 均为0,无法用来计算桥联矩阵元素。为此,将坐标旋转 45° 得最大剪应力。

纤维平均应力:

$$\overline{\sigma}_{xy}^f = \frac{4(C_{22}^f - C_{23}^f)C_{22}^m \sigma_0}{C_{22}^m(3C_{22}^f - 3C_{23}^f + C_{22}^m) - C_{23}^m(C_{22}^f - C_{23}^f + C_{23}^m)}, \quad (13)$$

$$\overline{\sigma}_{xz}^f = \overline{\sigma}_{yz}^f = 0, \quad (14)$$

C_{ij}^f 和 C_{ij}^m 分别是纤维和基体的刚度矩阵元素。

基体平均应力:

$$\overline{\sigma}_{xy}^m = \sigma_0, \quad (15)$$

$$\overline{\sigma}_{xz}^m = \overline{\sigma}_{yz}^m = 0. \quad (16)$$

2) 轴向剪切(y 截面)

纤维平均应力:

$$\overline{\sigma}_{xy}^f = \overline{\sigma}_{xz}^f = 0, \quad (17)$$

$$\overline{\sigma}_{yz}^f = \frac{2G_{12}^f \sigma_0}{G_{12}^f + G_{12}^m}. \quad (18)$$

基体平均应力:

$$\overline{\sigma}_{xy}^m = \overline{\sigma}_{xz}^m = 0, \quad (19)$$

$$\overline{\sigma}_{yz}^m = \sigma_0. \quad (20)$$

3) 轴向剪切(x 截面)

纤维平均应力:

$$\overline{\sigma}_{xy}^f = \overline{\sigma}_{yz}^f = 0, \quad (21)$$

$$\overline{\sigma_{xz}^f} = \frac{2G_{12}^f \sigma_0}{C_{12}^f + C_{12}^m}. \quad (22)$$

基体平均应力:

$$\overline{\sigma_{xy}^m} = \overline{\sigma_{yz}^m} = 0, \quad (23)$$

$$\overline{\sigma_{xz}^m} = \sigma_0. \quad (24)$$

4) 轴向拉伸

纤维平均应力:

$$\overline{\sigma_z^f} = \frac{(2C_{12}^f C_{12}^m (C_{23}^m - C_{22}^m) - 2C_{12}^{f2} (C_{22}^m + C_{23}^m)) \sigma_0}{(C_{22}^f + C_{23}^f + C_{22}^m - C_{23}^m) (C_{11}^m (C_{22}^m + C_{23}^m) - 2(C_{12}^m)^2)} + \frac{C_{11}^f \sigma_0 (C_{22}^f + C_{23}^f + C_{22}^m - C_{23}^m) (C_{22}^m + C_{23}^m)}{(C_{22}^f + C_{23}^f + C_{22}^m - C_{23}^m) (C_{11}^m (C_{22}^m + C_{23}^m) - 2(C_{12}^m)^2)}, \quad (25)$$

$$\overline{\sigma_x^f} = \frac{C_{12}^f \sigma_0 (C_{22}^m - C_{23}^m) (C_{22}^m + C_{23}^m)}{(C_{22}^f + C_{23}^f + C_{22}^m - C_{23}^m) (C_{11}^m (C_{22}^m + C_{23}^m) - 2(C_{12}^m)^2)} - \frac{C_{12}^m \sigma_0 (C_{22}^f + C_{23}^f) (C_{22}^m - C_{23}^m)}{(C_{22}^f + C_{23}^f + C_{22}^m - C_{23}^m) (C_{11}^m (C_{22}^m + C_{23}^m) - 2(C_{12}^m)^2)}, \quad (26)$$

$$\overline{\sigma_y^f} = \frac{C_{12}^f \sigma_0 (C_{22}^m - C_{23}^m) (C_{22}^m + C_{23}^m)}{(C_{22}^f + C_{23}^f + C_{22}^m - C_{23}^m) (C_{11}^m (C_{22}^m + C_{23}^m) - 2(C_{12}^m)^2)} - \frac{C_{12}^m \sigma_0 (C_{22}^f + C_{23}^f) (C_{22}^m - C_{23}^m)}{(C_{22}^f + C_{23}^f + C_{22}^m - C_{23}^m) (C_{11}^m (C_{22}^m + C_{23}^m) - 2(C_{12}^m)^2)}. \quad (27)$$

基体平均应力:

$$\overline{\sigma_z^m} = \sigma_0, \quad (28)$$

$$\overline{\sigma_x^m} = 0, \quad (29)$$

$$\overline{\sigma_y^m} = 0. \quad (30)$$

5) 双轴横向拉伸

纤维平均应力:

$$\overline{\sigma_z^f} = \frac{4C_{12}^f C_{22}^m \sigma_0}{(C_{22}^f + C_{23}^f + C_{22}^m - C_{23}^m) (C_{22}^m + C_{23}^m)}, \quad (31)$$

$$\overline{\sigma_x^f} = \frac{(C_{22}^f + C_{23}^f + C_{32}^f + C_{33}^f) C_{22}^m \sigma_0}{(C_{22}^f + C_{23}^f + C_{22}^m - C_{23}^m) (C_{22}^m + C_{23}^m)}, \quad (32)$$

$$\overline{\sigma_y^f} = \frac{(C_{22}^f + C_{23}^f + C_{32}^f + C_{33}^f) C_{22}^m \sigma_0}{(C_{22}^f + C_{23}^f + C_{22}^m - C_{23}^m) (C_{22}^m + C_{23}^m)}. \quad (33)$$

基体平均应力:

$$\overline{\sigma_z^m} = \frac{2C_{12}^m \sigma_0}{C_{22}^m + C_{23}^m}, \quad (34)$$

$$\overline{\sigma_x^m} = \sigma_0, \quad (35)$$

$$\overline{\sigma_y^m} = \sigma_0. \quad (36)$$

6) 单轴横向拉伸

纤维平均应力:

$$\overline{\sigma_z^f} = \frac{2C_{12}^f C_{22}^m \sigma_0}{(C_{22}^f + C_{23}^f + C_{22}^m - C_{23}^m)(C_{22}^m + C_{23}^m)}, \quad (37)$$

$$\overline{\sigma_x^f} = \frac{1}{2} \left(\frac{4(C_{22}^f - C_{23}^f) C_{22}^m \sigma_0}{(C_{22}^m)^2 + 6C_{22}^m C_{23}^f - C_{23}^m (C_{23}^m + 2C_{23}^f)} + \frac{(C_{22}^f + C_{23}^f + C_{32}^f + C_{33}^f) C_{22}^m \sigma_0}{(C_{22}^f + C_{23}^f + C_{22}^m - C_{23}^m)(C_{22}^m + C_{23}^m)} \right), \quad (38)$$

$$\overline{\sigma_y^f} = \frac{1}{2} \left(\frac{4(C_{23}^f - C_{22}^f) C_{22}^m \sigma_0}{(C_{22}^m)^2 + 6C_{22}^m C_{23}^f - C_{23}^m (C_{23}^m + 2C_{23}^f)} + \frac{(C_{22}^f + C_{23}^f + C_{32}^f + C_{33}^f) C_{22}^m \sigma_0}{(C_{22}^f + C_{23}^f + C_{22}^m - C_{23}^m)(C_{22}^m + C_{23}^m)} \right). \quad (39)$$

基体平均应力:

$$\overline{\sigma_z^m} = \frac{2C_{12}^m \sigma_0}{C_{22}^m + C_{23}^m}, \quad (40)$$

$$\overline{\sigma_x^m} = \sigma_0, \quad (41)$$

$$\overline{\sigma_y^m} = 0. \quad (42)$$

3 桥联矩阵

3.1 矩阵求解

桥联矩阵可分成两个互不耦合的子块,每个子块只与正应力或剪应力有关,据此对两个子块分别求解.

1) 正应力相关的矩阵

该子块只与正应力相关,略去剪应力分量,将单轴横向拉伸、双轴横向拉伸及轴向拉伸的应力场代入桥联方程如下:

$$\begin{bmatrix} \overline{\sigma_{z1}^m} & \overline{\sigma_{z2}^m} & \overline{\sigma_{z3}^m} \\ \overline{\sigma_{x1}^m} & \overline{\sigma_{x2}^m} & \overline{\sigma_{x3}^m} \\ \overline{\sigma_{y1}^m} & \overline{\sigma_{y2}^m} & \overline{\sigma_{y3}^m} \end{bmatrix} = \begin{bmatrix} A_{11} & A_{12} & A_{13} \\ A_{21} & A_{22} & A_{23} \\ A_{31} & A_{32} & A_{33} \end{bmatrix} \begin{bmatrix} \overline{\sigma_{z1}^f} & \overline{\sigma_{z2}^f} & \overline{\sigma_{z3}^f} \\ \overline{\sigma_{x1}^f} & \overline{\sigma_{x2}^f} & \overline{\sigma_{x3}^f} \\ \overline{\sigma_{y1}^f} & \overline{\sigma_{y2}^f} & \overline{\sigma_{y3}^f} \end{bmatrix}. \quad (43)$$

经符号运算和化简,得桥联矩阵元素为

$$A_{11} = \frac{E_{11}^m (E_{11}^m - E_{22}^m \mu_{12}^f \mu_{12}^m)}{E_{11}^f (E_{11}^m - E_{22}^m (\mu_{12}^m)^2)}, \quad (44)$$

$$A_{12} = A_{13} = \frac{E_{11}^m (E_{11}^f \mu_{12}^m (1 + \mu_{23}^m) - 2E_{11}^m \mu_{12}^f)}{2E_{11}^f (E_{11}^m - E_{22}^m (\mu_{12}^m)^2)} + \frac{E_{11}^m E_{22}^m \mu_{12}^m (1 - \mu_{23}^f)}{2E_{22}^f (E_{11}^m - E_{22}^m (\mu_{12}^m)^2)}, \quad (45)$$

$$A_{21} = A_{31} = \frac{E_{11}^m E_{22}^m (\mu_{12}^m - \mu_{12}^f)}{2E_{11}^f (E_{11}^m - E_{22}^m (\mu_{12}^m)^2)}, \quad (46)$$

$$A_{22} = A_{33} = \frac{E_{11}^m(5E_{22}^f + 3E_{22}^m + E_{22}^f\mu_{23}^m - E_{22}^m\mu_{23}^f)}{8E_{22}^f(E_{11}^m - E_{22}^m(\mu_{12}^m)^2)} + \frac{E_{22}^m(-4E_{11}^m\mu_{12}^f\mu_{12}^m - 4E_{11}^f(\mu_{12}^m)^2)}{8E_{11}^f(E_{11}^m - E_{22}^m(\mu_{12}^m)^2)}, \quad (47)$$

$$A_{23} = A_{32} = \frac{E_{11}^m(-E_{22}^f + E_{22}^m - 3E_{22}^m\mu_{23}^f + 3E_{22}^f\mu_{23}^m)}{8E_{22}^f(E_{11}^m - E_{22}^m(\mu_{12}^m)^2)} + \frac{E_{22}^m(-4E_{11}^m\mu_{12}^f\mu_{12}^m + 4E_{11}^f(\mu_{12}^m)^2)}{8E_{11}^f(E_{11}^m - E_{22}^m(\mu_{12}^m)^2)}, \quad (48)$$

其中 $E_{11}^f, E_{22}^f, \mu_{12}^f, \mu_{23}^f$ 和 $E_{11}^m, E_{22}^m, \mu_{12}^m, \mu_{23}^m$ 分别是纤维和基体的轴向(沿纤维轴向)模量、横向模量、轴向 Poisson(泊松)比、横向 Poisson 比。

2) 剪应力相关的矩阵

同理,只需考虑纤维和基体中的剪应力项,对应的加载分别为横向剪切和两个方向的轴向剪切.代入桥联方程,得到

$$\begin{bmatrix} \overline{\sigma_{xy1}^m} & \overline{\sigma_{xy2}^m} & \overline{\sigma_{xy3}^m} \\ \overline{\sigma_{xz1}^m} & \overline{\sigma_{xz2}^m} & \overline{\sigma_{xz3}^m} \\ \overline{\sigma_{yz1}^m} & \overline{\sigma_{yz2}^m} & \overline{\sigma_{yz3}^m} \end{bmatrix} = \begin{bmatrix} A_{44} & A_{45} & A_{46} \\ A_{54} & A_{55} & A_{56} \\ A_{64} & A_{65} & A_{66} \end{bmatrix} \begin{bmatrix} \overline{\sigma_{xy1}^f} & \overline{\sigma_{xy2}^f} & \overline{\sigma_{xy3}^f} \\ \overline{\sigma_{xz1}^f} & \overline{\sigma_{xz2}^f} & \overline{\sigma_{xz3}^f} \\ \overline{\sigma_{yz1}^f} & \overline{\sigma_{yz2}^f} & \overline{\sigma_{yz3}^f} \end{bmatrix}. \quad (49)$$

解出各桥联矩阵元素如下:

$$A_{44} = \frac{E_{22}^f(3E_{11}^m - 4E_{22}^m(\mu_{12}^m)^2 - E_{11}^m\mu_{23}^m) + E_{11}^mE_{22}^f(1 + \mu_{23}^f)}{4E_{22}^f(E_{11}^m - E_{22}^m(\mu_{12}^m)^2)}, \quad (50)$$

$$A_{55} = A_{66} = \frac{G_{12}^f + G_{12}^m}{2G_{12}^f}, \quad (51)$$

$$A_{45} = A_{46} = A_{54} = A_{56} = A_{64} = A_{65} = 0, \quad (52)$$

其中 G_{12}^f 和 G_{12}^m 是纤维和基体的轴向剪切模量。

3.2 与 Eshelby 方法对比

为了验证本文所求桥联矩阵的准确性,考虑基于 Eshelby 等效夹杂的 Mori-Tanaka 桥联矩阵^[25]如下:

$$[A_{ij}] = [K_{ij}^m](\mathbf{I} + [L_{ij}][S_{ij}^m])([K_{ij}^f] - [K_{ij}^m])[S_{ij}^f]. \quad (53)$$

由于两者的研究对象相同,根据弹性力学解的唯一性原理,两者得到的桥联矩阵必然完全一致,即式(53)与式(10)相同.但在式(53)中, L_{ij} 为 Eshelby 张量,在基体为横观各向同性的情况下,可根据文献[26]的公式,通过数值积分得到,进而由式(53)确定桥联矩阵.称后一种方法得到的桥联矩阵为 Eshelby 方法.取表 1 组分材料参数,两种不同方法计算的桥联矩阵非 0 元素列入表 2.

表 1 纤维基体性能参数

Table 1 Fiber matrix performance parameters

	E_{11}^i /GPa	E_{22}^i /GPa	G_{12}^i /GPa	μ_{12}^i	μ_{23}^i
$i = f$	276	19	27	0.2	0.36
$i = m$	4.08	3.2	1.48	0.38	0.35

表2 与 Eshelby 张量得到的 Mori-Tanaka 桥联矩阵比较表

Table 2 Comparison with the Mori-Tanaka bridging matrix obtained from the Eshelby tensor

matrix element	Eshelby method	the present method
A_{11}	0.015 675 1	0.015 676 9
A_{22}	0.752 481	0.752 483
A_{33}	0.752 485	0.752 483
A_{12}	0.309 019	0.309 022
A_{13}	0.309 022	0.309 022
A_{21}	0.001 173 81	0.001 176 75
A_{23}	0.068 506 9	0.068 512
A_{31}	0.001 174 78	0.001 176 75
A_{32}	0.068 510 6	0.068 512
A_{44}	0.683 956	0.683 971
A_{55}	0.527 411	0.527 407
A_{66}	0.527 404	0.527 407

表2证实,不考虑数值积分的误差,两种途径所求桥联矩阵完全相同,但本文得到的是封闭解析公式。

4 等效弹性常数

桥联矩阵的一个重要应用是计算复合材料的等效弹性常数,单向复合材料的柔度矩阵由式(9)给出,据此,导出横观各向同性基体复合材料的5个等效弹性常数的解析表达式如下:

$$E_{11} = \frac{1}{S_{11}} = [(A_{11} + A_{22} + A_{33})V_f V_m + (A_{11}(A_{22} + A_{32}) - 2A_{12}A_{21})V_m^2 + V_f^2] / [V_f V_m(2A_{21}(S_{12}^m - S_{12}^f) + (A_{22} + A_{32})S_{11}^f + A_{11}S_{11}^m) + (A_{11}(A_{22} + A_{32}) - 2A_{12}A_{21})S_{11}^m V_m^2 + S_{11}^f V_f^2], \quad (54)$$

$$E_{22} = \frac{1}{S_{22}} = [(V_f + (A_{22} - A_{23})V_m)(V_f^2 + (A_{11} + A_{22} + A_{23})V_f V_m + (A_{11}(A_{22} + A_{23}) - 2A_{12}A_{21})V_m^2)] / [S_{22}^f V_f^3 + S_{22}^f V_f(m_1 + m_2) + V_m A_{12}(V_f^2(S_{12}^m - S_{12}^f) - m_3 + m_4) - V_m(V_f + A_{11}V_m)(m_5 - m_6)], \quad (55)$$

$$G_{12} = \frac{1}{S_{66}} = \frac{(V_f + V_m A_{66})G_{12}^f G_{12}^m}{V_f G_{12}^m + V_m A_{66} G_{12}^f}, \quad (56)$$

$$G_{23} = \frac{1}{S_{44}} = \frac{(V_f + V_m A_{44})G_{23}^f G_{23}^m}{V_f G_{23}^m + V_m A_{44} G_{23}^f}, \quad (57)$$

$$\mu_{12} = -\frac{S_{12}}{S_{11}} = [A_{12}V_m(V_f(S_{11}^f - S_{11}^m) + 2A_{21}V_m S_{12}^m) - (V_f + A_{11}V_m)(V_f S_{12}^f + (A_{22} + A_{32})V_m S_{12}^m)] / [V_f^2 S_{11}^f + (-2A_{12}A_{21} + A_{11}(A_{22} + A_{32}))V_m^2 S_{11}^m + V_f V_m((A_{22} + A_{32})S_{11}^f + A_{11}S_{11}^m + 2A_{21}(S_{12}^m - S_{12}^f))], \quad (58)$$

其中

$$\begin{cases} m_1 = V_f V_m (A_{11} + A_{22}), m_2 = V_m^2 (A_{11} A_{22} - A_{12} A_{21}), \\ m_3 = V_f V_m ((A_{22} - A_{23})(S_{12}^f - S_{12}^m) + A_{21}(S_{22}^m + S_{23}^m - S_{23}^f)), \\ m_4 = 2A_{21}(A_{23} - A_{22})S_{22}^m V_m^2, m_5 = A_{23}(S_{23}^f - S_{23}^m)V_f + A_{23}^2 S_{22}^m V_m, \\ m_6 = A_{22} S_{22}^m (V_f + A_{22} V_m). \end{cases} \quad (59)$$

需要指出的是,式(56)与文献[16]的结果完全相同.但文献[16]仅仅导出了面内剪切模量的封闭公式,本文在这里补齐了余下的4个公式.

5 桥联模型

虽然 CCA 模型(或 Mori-Tanaka 模型,对单向复合材料两者等价)能够给出桥联矩阵以及5个等效复合材料弹性常数的显式公式,但其表达式仍略嫌复杂.此外,将退化的二维 Mori-Tanaka 桥联矩阵,即

$$[A_{ij}] = \begin{bmatrix} A_{11} & A_{12} & 0 \\ A_{21} & A_{22} & 0 \\ 0 & 0 & A_{66} \end{bmatrix}, \quad (60)$$

代入式(9),其中纤维和基体的柔度矩阵亦是二维矩阵,容易证明,所得到的复合材料柔度矩阵不对称.事实上,将式(60)代入式(9),根据对称性条件:

$$S_{21} = S_{12}, \quad (61)$$

解出^[20]

$$A_{12} = \frac{(S_{12}^f - S_{12}^m)(A_{22} - A_{11}) + (S_{22}^m - S_{22}^f)A_{21}}{S_{11}^m - S_{11}^f}. \quad (62)$$

显而易见,将式(44)、(46)、(47)代入式(62)右边,所得与式(45)的 A_{12} 不等.因此,有必要对 CCA 模型的桥联矩阵进行修正.

分别将桥联模型^[20]桥联矩阵元素中的基体模量用横观各向同性参数置换,得到修正公式如下(将桥联模型的桥联矩阵元素用小写 a_{ij} 表示):

$$a_{11} = E_{11}^m / E_{11}^f, \quad (63)$$

$$a_{22} = a_{33} = a_{44} = \beta + (1 - \beta) \frac{E_{22}^m}{E_{22}^f}, \quad 0 < \beta < 1, \quad (64)$$

$$a_{55} = a_{66} = \alpha + (1 - \alpha) \frac{G_{12}^m}{G_{12}^f}, \quad 0 < \alpha < 1, \quad (65)$$

$$a_{12} = a_{13} = \frac{S_{12}^f - S_{12}^m}{S_{11}^f - S_{11}^m} (a_{11} - a_{22}), \quad (66)$$

其余 a_{ij} 均为0,式中 β 和 α 分别称为桥联参数,是可调参数,取值范围一般在0.3~0.6之间^[20],用以表征不同复合材料因纤维排列及截面形状不同导致的个体差异,可通过实验确定(将基于式(64)及(65)预报的复合材料横向及面内剪切模量与测试的模量对比,调整相应的参数).对树脂基复合材料,综合对比发现,取 $\beta = \alpha = 0.3$ 与实验之间的整体误差最小,精度高于许多其他细观力学模型包括 Mori-Tanaka 方法、广义自洽法、广义胞元法、有限元等方法的计算精度^[27].因此,当缺少实验数据时,建议取 $\beta = \alpha = 0.3$.对比式(65)和(62)可知,由桥联模型计算

的复合材料柔度矩阵,无论平面还是三维情况下都对称。

需要说明的是,桥联模型可由 CCA 模型的桥联矩阵略去高阶小量后得到。为简单起见,假定纤维和基体均为各向同性,再取一组典型纤维和基体材料组合的 Poisson 比 $\mu_f = 0.22, \mu_m = 0.35$, 对比式(44)~(48)、(50)~(52)和(63)~(66),有

$$A_{11} = \frac{E^m(1 - \mu^f \mu^m)}{E^f(1 - \mu^f \mu^f)} = 1.052 \frac{E^m}{E^f} \approx \frac{E^m}{E^f} = a_{11}, \quad (67)$$

$$A_{21} = A_{31} = \frac{E^m(\mu^m - \mu^f)}{2E^f(1 - (\mu^m)^2)} = 0.074 \frac{E^m}{E^f} \approx 0 = a_{21} = a_{31}, \quad (68)$$

$$A_{22} = A_{33} = \frac{E^m(\mu^f + 4\mu^f \mu^m - 3) + E^f(4(\mu^m)^2 - \mu^m - 5)}{8E^f((\mu^m)^2 - 1)} = 0.69 + 0.35 \frac{E^m}{E^f} \approx \beta + (1 - \beta) \frac{E^m}{E^f} = a_{22} = a_{33}, \quad (69)$$

$$A_{44} = \frac{E^m(1 + \mu^f) + E^f(3 - \mu^m - 4(\mu^m)^2)}{4E^f(1 - (\mu^m)^2)} = 0.62 + 0.35 \frac{E^m}{E^f} \approx \beta + (1 - \beta) \frac{E^m}{E^f} \approx A_{22} \approx a_{22}, \quad (70)$$

$$A_{32} = \frac{E^f(3\mu^m - 1 + 4(\mu^m)^2) + E^m(1 - 3\mu^f - 4\mu^f \mu^m)}{8E^f(1 - (\mu^m)^2)} = 0.077 + 0.0046 \frac{E^m}{E^f} \approx 0 = a_{32}, \quad (71)$$

$$A_{55} = A_{66} = \frac{G_{12}^f + G_{12}^m}{2G_{12}^f} = \alpha + (1 - \alpha) \frac{G^m}{G_{12}^f} = a_{55} = a_{66}. \quad (72)$$

其中,式(68)和(71)成立,是因为基体模量 E^m 一般远小于纤维模量 E^f ; 式(69)和(70)成立是取 $\beta \approx 0.69$; 式(72)成立是取 $\alpha = 0.5$ 。从式(67)~(72)不难看出,除了桥联参数 β 和 α 的取值外,由 Mori-Tanaka-Eshelby 桥联矩阵元素简化得到桥联模型对应的桥联矩阵元素,所产生的舍入误差一般不超过 10% (假定 $E^m < E^f$)。

6 数值对比

由于问题的复杂性,迄今尚未从公开文献上找到横观各向同性基体单向复合材料弹性性能的实验数据。下面通过数值分析,说明基体材料性能变化对复合材料等效弹性常数的影响,分别对比了 CCA 模型和桥联模型的计算结果。组分材料参数取值如表 3,依据 CCA 模型和桥联模型求得的复合材料 5 个等效弹性常数随纤维含量 V_f 变化的结果分别如图 7~11 所示。

表 3 纤维基体性能参数

Table 3 Properties of fiber and matrix

	E_{11}^f/GPa	E_{22}^f/GPa	μ_{12}^f	μ_{23}^f	G_{12}^f/GPa	E_{11}^m/GPa	E_{22}^m/GPa	μ_{12}^m	μ_{23}^m	G_{12}^m/GPa
$E_{11}^m/E_{22}^m = 1$	225	15	0.2	0.07	15	4.08	4.08	0.35	0.35	1.48
$E_{11}^m/E_{22}^m = 2$	225	15	0.2	0.07	15	4.08	2.04	0.35	0.40	1.48
$E_{11}^m/E_{22}^m = 5$	225	15	0.2	0.07	15	4.08	0.816	0.35	0.40	1.48
$E_{11}^m/E_{22}^m = 10$	225	15	0.2	0.07	15	4.08	0.408	0.35	0.40	1.48

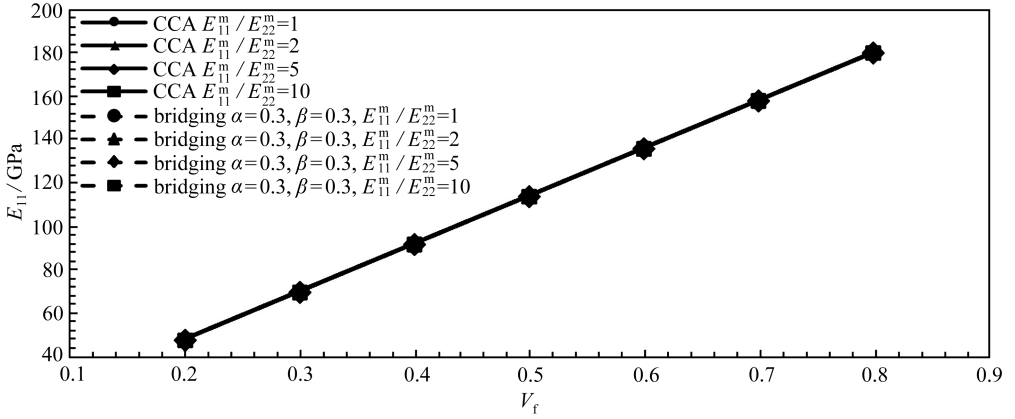


图 7(a) 不同基体性能参数下,CCA 模型和桥联模型 ($\alpha = 0.3, \beta = 0.3$) E_{11} 数值变化

Fig. 7(a) Predicted E_{11} vs. matrix property parameters with the CCA model and the bridging model ($\alpha = 0.3, \beta = 0.3$)

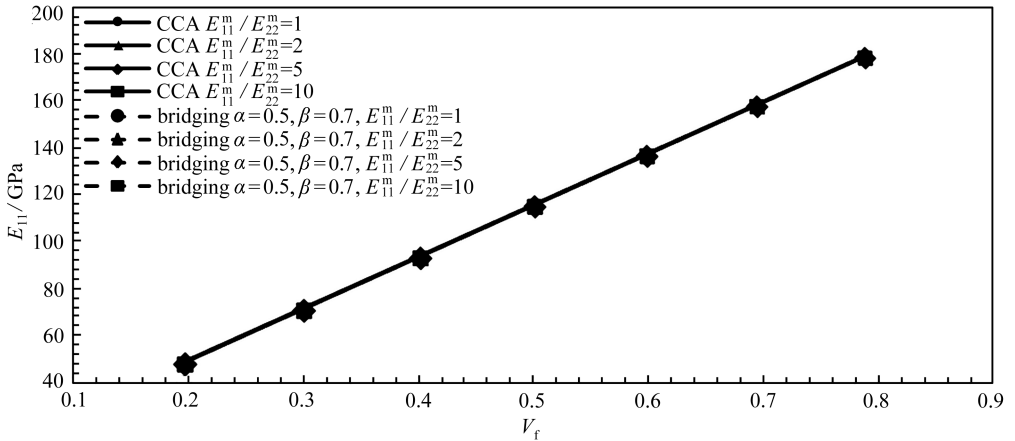


图 7(b) 不同基体性能参数下,CCA 模型和桥联模型 ($\alpha = 0.5, \beta = 0.7$) E_{11} 数值变化

Fig. 7(b) Predicted E_{11} vs. matrix property parameters with the CCA model and the bridging model ($\alpha = 0.5, \beta = 0.7$)

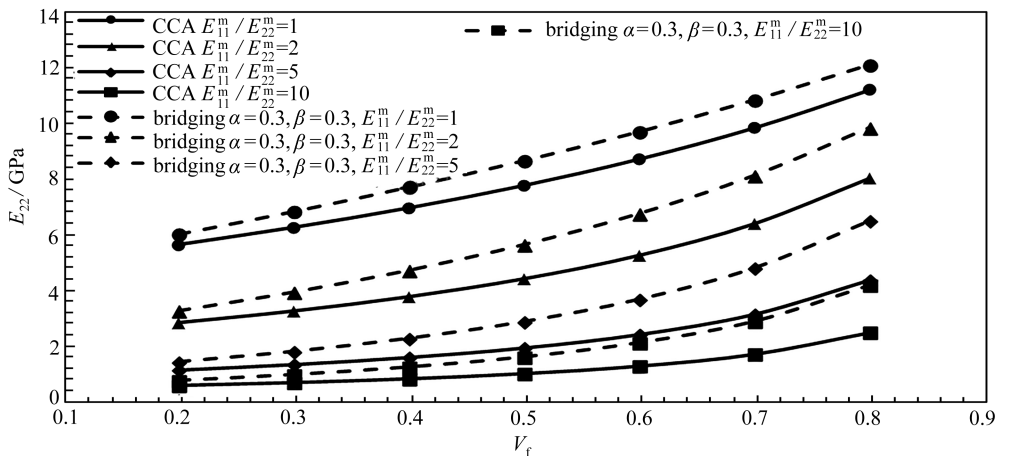


图 8(a) 不同基体性能参数下,CCA 模型和桥联模型 ($\alpha = 0.3, \beta = 0.3$) E_{22} 数值变化

Fig. 8(a) Predicted E_{22} vs. matrix property parameters with the CCA model and the bridging model ($\alpha = 0.3, \beta = 0.3$)

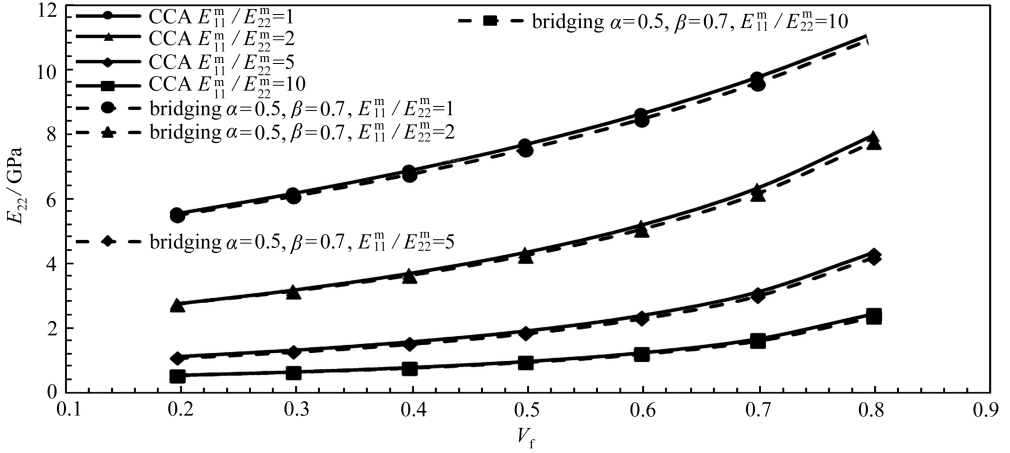


图 8(b) 不同基体性能参数下,CCA 模型和桥联模型 ($\alpha = 0.5, \beta = 0.7$) E_{22} 数值变化

Fig. 8(b) Predicted E_{22} vs. matrix property parameters with the CCA model and the bridging model ($\alpha = 0.5, \beta = 0.7$)

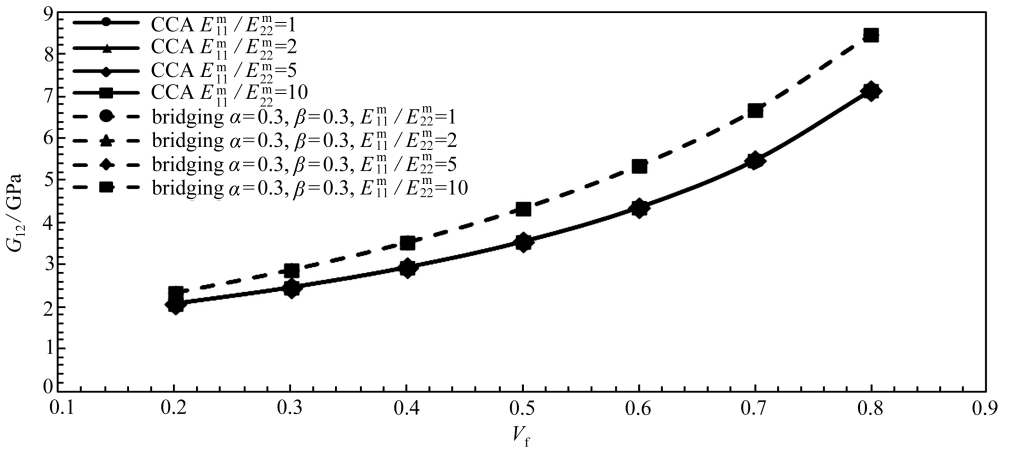


图 9(a) 不同基体性能参数下,CCA 模型和桥联模型 ($\alpha = 0.3, \beta = 0.3$) G_{12} 数值变化

Fig. 9(a) Predicted G_{12} vs. matrix property parameters with the CCA model and the bridging model ($\alpha = 0.3, \beta = 0.3$)

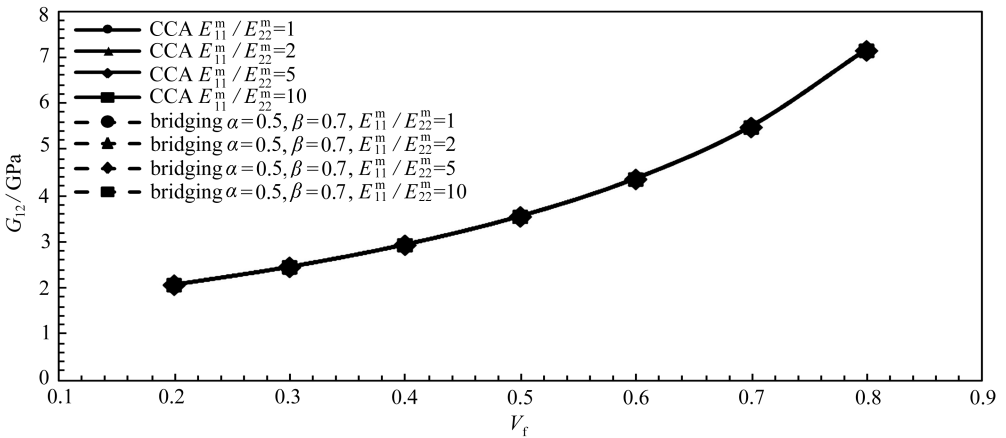


图 9(b) 不同基体性能参数下,CCA 模型和桥联模型 ($\alpha = 0.5, \beta = 0.7$) G_{12} 数值变化

Fig. 9(b) Predicted G_{12} vs. matrix property parameters with the CCA model and the bridging model ($\alpha = 0.5, \beta = 0.7$)

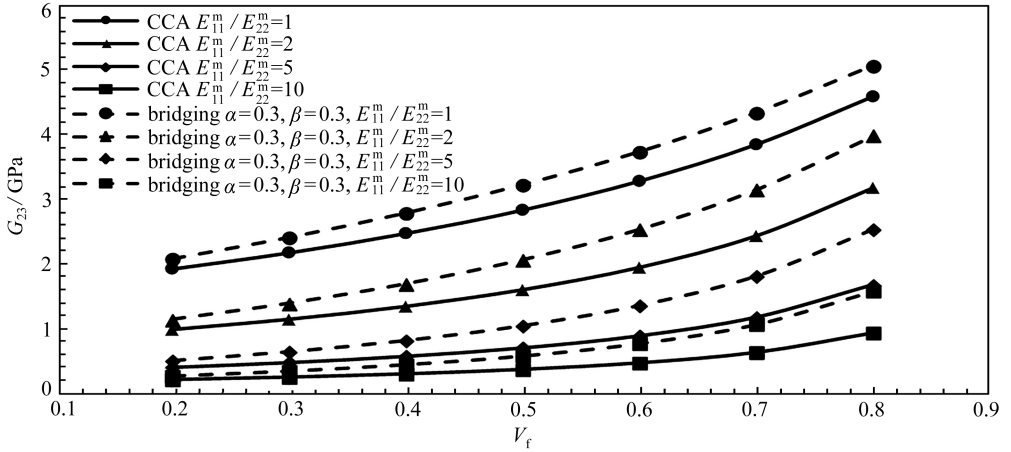


图 10(a) 不同基体性能参数下,CCA 模型和桥联模型 ($\alpha = 0.3, \beta = 0.3$) G_{23} 数值变化

Fig. 10(a) Predicted G_{23} vs. matrix property parameters with the CCA model and the bridging model ($\alpha = 0.3, \beta = 0.3$)

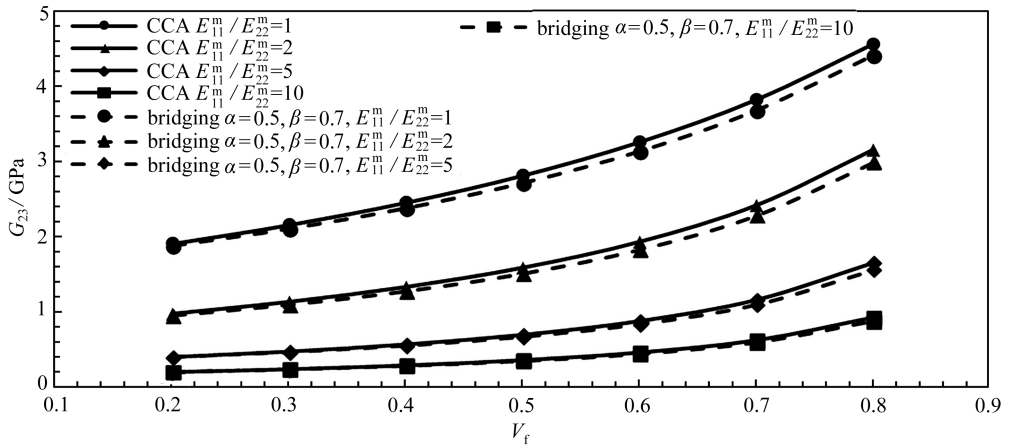


图 10(b) 不同基体性能参数下,CCA 模型和桥联模型 ($\alpha = 0.5, \beta = 0.7$) G_{23} 数值变化

Fig. 10(b) Predicted G_{23} vs. matrix property parameters with the CCA model and the bridging model ($\alpha = 0.5, \beta = 0.7$)

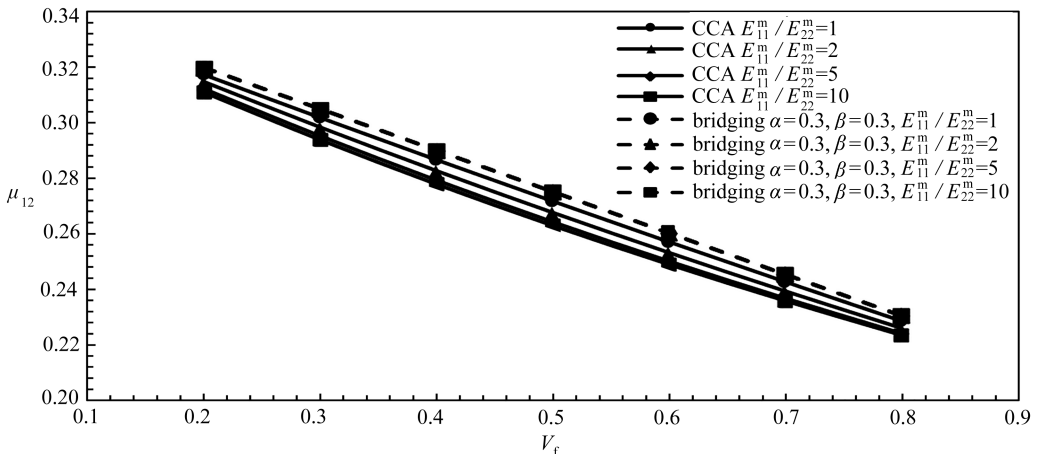


图 11(a) 不同基体性能参数下,CCA 模型和桥联模型 ($\alpha = 0.3, \beta = 0.3$) μ_{12} 数值变化

Fig. 11(a) Predicted μ_{12} vs. matrix property parameters with the CCA model and the bridging model ($\alpha = 0.3, \beta = 0.3$)

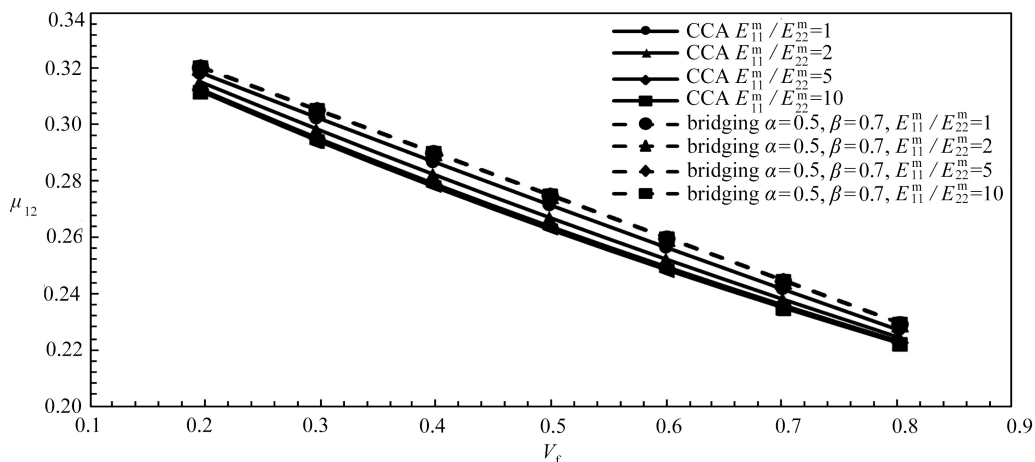


图 11(b) 不同基体性能参数下, CCA 模型和桥联模型 ($\alpha = 0.5, \beta = 0.7$) μ_{12} 数值变化

Fig. 11(b) Predicted μ_{12} vs. matrix property parameters with the CCA model and the bridging model ($\alpha = 0.5, \beta = 0.7$)

从上述图中的数据对比,可得出如下结论:

- 1) 桥联模型可通过改变桥联参数 β 和 α , 来调整横向模量 E_{22}, G_{23} 以及轴向剪切模量 G_{12} 的预报;
- 2) 当桥联参数取 $\beta = 0.7, \alpha = 0.5$ 时, 桥联模型预报的等效弹性常数与本文所导的 CCA 模型等效弹性常数计算值基本一致;
- 3) 等效弹性常数 $E_{11}, E_{22}, G_{12}, G_{23}$ 随着 V_f 的增加而增加, 只有 μ_{12} 随 V_f 的增加而减小;
- 4) 基体性能不同, 对复合材料等效模量 E_{11}, G_{12}, μ_{12} 的影响不大 (假定纤维性能参数远高于基体), E_{11}, G_{12}, μ_{12} 各自数值接近相等, 而 E_{22}, G_{23} 的预报值之间差异显著。

7 结 论

- 1) 本文导出了基体为横观各向同性复合材料的 5 个弹性常数显式表达式。
- 2) 桥联参数取特定值, CCA 模型和桥联模型计算的横观各向同性基体复合材料的各弹性参数十分接近, 但桥联模型公式更简洁、应用更方便。
- 3) 基于本文结果和文献 [15] 的等效纤维方法, 可方便地计算纤维-界面-基体三相共存下的复合材料等效弹性常数。

参考文献 (References):

- [1] HASHIN Z. Analysis of composite materials: a survey [J]. *Journal of Applied Mechanics*, 1983, **50**(3): 481-505.
- [2] UPADHYAY A, SINGH R. Prediction of effective elastic modulus of biphasic composite materials [J]. *Modern Mechanical Engineering*, 2012, **2**(1): 6-13.
- [3] TSAI S W, HAHN H T. *Introduction to Composite Materials* [M]. Lancaster: Technomic Publishing Co, 1980.
- [4] BUDIANSKY B. On the elastic moduli of some heterogeneous materials [J]. *Journal of the Mechanics and Physics of Solids*, 1965, **13**(4): 223-227.
- [5] HILL R. A self-consistent mechanics of composite materials [J]. *Journal of the Mechanics and Physics of Solids*, 1965, **13**(4): 213-222.

- [6] KERNER E H. The elastic and thermo-elastic properties of composite media[J]. *Proceedings of the Physical Society Section B*, 1956, **69**(2): 807-808.
- [7] CHRISTENSEN R M, LO K H. Solutions for effective shear properties in three phase sphere and cylinder models[J]. *Journal of the Mechanics & Physics of Solids*, 1979, **27**(4): 315-330.
- [8] MORI T, TANAKA K. Average stress in matrix and average elastic energy of materials with-in-fitting inclusions[J]. *Acta Metallurgica*, 1973, **21**(5): 571-574.
- [9] CHAMIS C C. Mechanics of composite materials-past, present and future[J]. *Journal of Composites Technology & Research*, 1984, **11**(1): 3-14.
- [10] HUANG Z M. Simulation of the mechanical properties of fibrous composites by the bridging micromechanics model[J]. *Composites Part A*, 2001, **32**(2): 143-172.
- [11] BENVENISTE Y. Exact results for the local fields and the effective moduli of fibrous composites with thickly coated fibers[J]. *Journal of the Mechanics & Physics of Solids*, 2014, **71**(1): 219-238.
- [12] GOTKHINDI T P, SIMHA K R Y. Transverse elastic response of bundled coated cylinders[J]. *International Journal of Mechanical Sciences*, 2013, **76**: 70-85.
- [13] CHATZIGEORGIOU G, SEIDEL G D, LAGOUDAS D C. Effective mechanical properties of “fuzzy fiber” composites[J]. *Composites Part B: Engineering*, 2012, **43**(6): 2577-2593.
- [14] HASEGAWA H, KISAKI M. The stress field caused by a circular cylindrical inclusion in a transversely isotropic elastic solid[J]. *Journal of Applied Mechanics*, 2004, **70**(6): 825-831.
- [15] WANG Y C, HUANG Z M. Bridging tensor with an imperfect interface[J]. *European Journal of Mechanics A: Solids*, 2015, **56**: 73-91.
- [16] GREBENYUK S N. The shear modulus of a composite material with a transversely isotropic matrix and a fibre[J]. *Journal of Applied Mathematics & Mechanics*, 2014, **78**(2): 187-191.
- [17] ESHELBY J D. The determination of the elastic field of an ellipsoidal inclusion, and related problems[J]. *Proceedings of the Royal Society of London*, 1957, **241**(1226): 376-396.
- [18] ESHELBY J D. The elastic field outside an ellipsoidal inclusion[J]. *Proceedings of the Royal Society of London*, 1959, **252**(1271): 561-569.
- [19] WANG Y, HUANG Z. A new approach to a bridging tensor[J]. *Polymer Composites*, 2014, **36**(8): 1417-1431.
- [20] HUANG Z M, ZHOU Y X. *Strength of Fibrous Composites*[M]. Zhejiang: Zhejiang University Press, 2011.
- [21] CHEN T, DVORAK G J, BENVENISTE Y. Stress fields in composites reinforced by coated cylindrically orthotropic fibers[J]. *Mechanics of Materials*, 1990, **9**(1): 17-32.
- [22] CHENG S, CHEN D. On the stress distribution in laminae[J]. *Journal of Reinforce Plast & Compos*, 1988, **7**(2): 136-144.
- [23] BENVENISTE Y, DVORAK G J, CHEN T. Stress fields in composites with coated inclusions [J]. *Mechanics of Materials*, 1989, **7**(4): 305-317.
- [24] TIMOSHENKON S P, GOODIER J N. *Theory of Elasticity*[M]. New York: McGraw-Hill Book Company, 1970.
- [25] BENVENISTE Y. A new approach to the application of Mori-Tanaka’s theory in composite materials[J]. *Mechanics of Materials*, 1987, **6**(2): 147-157.
- [26] GAVAZZI A C, LAGOUDAS D C. On the numerical evaluation of Eshelby’s tensor and its application to elastoplastic fibrous composites[J]. *Computational Mechanics*, 1990, **7**(1): 13-

19.

- [27] HUANG Z M, ZHANG C C. A critical assessment on the predictability of 12 micromechanics models for stiffness and strength of UD composites[C]//21st International Conference on Composite Materials. Xi'an, China, 2017.

Effective Elastic Properties of Transversely Isotropic Matrix Based Composites

ZHANG Chunchun, WANG Yanchao, HUANG Zhengming

(School of Aerospace Engineering & Applied Mechanics,
Tongji University, Shanghai 200092, P.R.China)

(Contributed by HUANG Zhengming, M. AMM Editorial Board)

Abstract: One of the main objectives of micromechanics is to predict the effective elastic properties of composites. Most existent explicit micromechanics models are based on an assumption of isotropic matrices and on that only 2-phase constituent materials are involved. In reality, a composite may possess a 3rd interphase between the fiber and the matrix, which is generally transversely isotropic. Accordingly, the prediction of the elastic properties of a 3-phase composite can be achieved through the combination of 2 kinds of 2-phase composites, to which a micromechanics model with transversely isotropic matrix should be applicable. The explicit bridging tensor elements to correlate the internal stresses of a transversely isotropic matrix with those of a reinforcing fiber in a concentric cylinder assemblage (CCA) model were derived firstly. Then this obtained bridging tensor was used to deduce analytical formulae for all the 5 effective elastic moduli of the composite made with the transversely isotropic matrix. An extension of the bridging model applicable to fiber reinforced transversely isotropic matrix composites was achieved as well. With properly chosen bridging parameters, the predicted elastic moduli of the composite with the 2 models are quite close to each other.

Key words: micromechanics; effective elastic property; anisotropic matrix; bridging tensor; bridging model

Foundation item: The National Natural Science Foundation of China(11472192;11272238)

引用本文/Cite this paper:

张春春, 王艳超, 黄争鸣. 横观各向同性基体复合材料的等效弹性常数[J]. 应用数学和力学, 2018, 39(7): 750-765.

ZHANG Chunchun, WANG Yanchao, HUANG Zhengming. Effective elastic properties of transversely isotropic matrix based composites[J]. *Applied Mathematics and Mechanics*, 2018, 39(7): 750-765.